Published in final edited form as:
Lasers Surg Med. 2011 September ; 43(7): 676–685. doi:10.1002/lsm.21107.

IL-6 Potentiates Tumor Resistance to Photodynamic Therapy (PDT)

Craig M. Brackett, BS, **Barbara Owczarczak, BS**, **Kimberley Ramsey, BS**, **Patricia G. Maier, BS**, and **Sandra O. Gollnick, PhD***
Departments of Immunology and Cell Stress Biology, Roswell Park Cancer Institute, Buffalo, New York 14263

Abstract

Background and Objective—Photodynamic therapy (PDT) is an anticancer modality approved for the treatment of early disease and palliation of late stage disease. PDT of tumors results in the generation of an acute inflammatory response. The extent and duration of the inflammatory response is dependent upon the PDT regimen employed and is characterized by rapid induction of proinflammatory cytokines, such as IL-6, and activation and mobilization of innate immune cells. The importance of innate immune cells in long-term PDT control of tumor growth has been well defined. In contrast the role of IL-6 in long-term tumor control by PDT is unclear. Previous studies have shown that IL-6 can diminish or have no effect on PDT antitumor efficacy.

Study Design/Materials and Methods—In the current study we used mice deficient for IL-6, *Il6*$^{-/-}$, to examine the role of IL-6 in activation of antitumor immunity and PDT efficacy by PDT regimens known to enhance antitumor immunity.

Results—Our studies have shown that elimination of IL-6 had no effect on innate cell mobilization into the treated tumor bed or tumor draining lymph node (TDLN) and did not affect primary antitumor T-cell activation by PDT. However, IL-6 does appear to negatively regulate the generation of antitumor immune memory and PDT efficacy against murine colon and mammary carcinoma models. The inhibition of PDT efficacy by IL-6 appears also to be related to regulation of Bax protein expression. Increased apoptosis was observed following treatment of tumors in *Il6*$^{-/-}$ mice 24 hours following PDT.

Conclusions—The development of PDT regimens that enhance antitumor immunity has led to proposals for the use of PDT as an adjuvant treatment. However, our results show that the potential for PDT induced expression of IL-6 to enhance tumor survival following PDT must be considered.

Keywords

IL-6; PDT; T cell memory

INTRODUCTION

Photodynamic therapy (PDT) is a FDA-approved anticancer modality for the treatment of early disease and palliation of late stage malignancies [1,2]. The treatment involves the

*Corresponding to: Photodynamic Therapy Center, Roswell Park Cancer Institute, Elm & Carlton Streets, Buffalo, NY 14263. sandra.gollnick@roswellpark.org.

systemic or topical application of a photoreactive drug known as a photosensitizer, which is inert until activated by light of a specific wavelength [3]. Light activation of the photosensitizer leads to the production of reactive oxygen species and direct tumor cell death. PDT also induces secondary events, including microvascular disruption, that contribute significantly to the long-term tumor growth control by PDT [2].

PDT induced tumor cell death and microvascular disruption can lead to increased local and systemic expression of proinflammatory cytokines and activation of innate immune cells [2,4–6] that culminates in the generation of T-cell mediated antitumor immunity [6,7]. The extent to which PDT stimulates inflammation and antitumor immunity is strongly influenced by both fluence and fluence rate [6,8,9]. The activation of innate cells is critical to efficacy of PDT regimens that induce inflammation [10–12] and antitumor immunity [8]. PDT enhancement of antitumor immunity has the potential to expand the use of PDT beyond that of a local treatment into one that can combat distant disease [13]. Unfortunately, acute inflammation can transit to chronic inflammation that may result in the generation of an immuno-suppressed, protumorigenic environment [14]. Therefore, greater understanding of the role of inflammation in PDT-induction of antitumor immunity is needed prior to development of clinical PDT protocols that induce antitumor immunity.

In contrast to the role of innate cells, the role of PDT induced proinflammatory cytokines in PDT efficacy and induction of antitumor immunity is poorly understood. Interleukin 6 (IL-6) is a prototypic inflammatory cytokine that plays a major role in the resolution of inflammation and transition to T-cell mediated antitumor immunity [15]. Multiple clinical and preclinical studies have shown that PDT of tumors leads to increased IL-6 expression [8,16–20]. Blockade of IL-6 activity has been shown to have either no effect [19,21] or to diminish PDT efficacy [22]. None of these reports examined the influence of IL-6 on PDT induction of antitumor immunity.

IL-6 is an important regulator of T-cell proliferation, differentiation, and survival [15]; PDT induced antitumor immunity is dependent upon T cells [7]. Therefore, we predicted that PDT induction of IL-6 would contribute to induction of antitumor immunity by PDT and that loss of IL-6 would impair PDT efficacy in PDT regimens that induce antitumor immunity. However, in this report we demonstrate that IL-6 does not contribute to the initial activation of antitumor-immunity by PDT. T-cell activation postPDT was similar in wild type and IL-6 deficient strains of mice; although immune memory was enhanced following PDT of Colo26 tumor bearing $IL6^{-/-}$ mice. Furthermore, both the inhibition of tumor growth and the tumor cure rate following PDT were enhanced in the absence of IL-6 in colon and mammary carcinoma models. Subsequent study showed that IL-6 appears to impair expression of the proapoptotic protein Bax post-PDT.

MATERIALS AND METHODS

Animals and Tumor Models

Pathogen-free BALB/c/ByJ mice were obtained from the National Cancer Institute. CByJ.129S2(B6)-$Il6^{tm1Kopf}$/J mice were obtained from Jackson Laboratories and bred in the Roswell Park Cancer Institute Department of Laboratory Animal Resources. CByJ.129S2(B6)-$Il6^{tm1Kopf}$/J (hereafter referred to as $IL6^{-/-}$) mice were generated at Jackson Laboratories and exhibit similar characteristics to $IL6^{-/-}$ mice on the C57BL/6 background [23,24]. SCID mice were obtained from the Roswell Park Department of Laboratory Animal Resources. Bone marrow chimeras were generated by treatment of $IL6^{-/-}$ and BALB/c mice with two doses of 6 Gy irradiation 24 hours apart. Six hours after the second dose of irradiation the mice were rescued with 4×10^6 bone marrow cells injected intravenously. The bone marrow cells were harvested by flushing femurs and tibias with PBS. Red blood

cells (RBCs) were lysed and the cells were resuspended in physiological saline. The cell suspension was filtered immediately before injection. All mice used in experimental procedures were female and were housed in microisolator cages in a laminar flow unit under ambient light. The RPCI Institutional Animal Care and Use Committee approved all procedures carried out in this study.

Colon 26 murine colon carcinoma cells [8] and 4T1 murine mammary carcinoma cells [25] were grown in RPMI 1640 supplemented with 10% FBS and antibiotics. All cells were cultured in a humidified atmosphere of 5% CO_2 in air at 37°C.

Photodynamic Therapy

Six-week to 10-week old animals were inoculated intradermally on the shoulder or abdominal mammary fat pad with live tumor cells (10^6 Colo 26 or 10^5 4T1 cells). When the tumors had reached 5 mm × 5 mm, the mice were injected i.v. with clinical-grade, pyrogen-free 2-[1-hexyloxyethyl]-2-devinyl pyropheophorbide-a (HPPH; 0.4 mM; Roswell Park Pharmacy, Buffalo, NY), or porfimer sodium (PII; 7.5 mg/kg; Axcan Pharma, Birmingham, AL). After 18–24 hours, tumors were exposed to 635 nm (HPPH) or 630 nm (PII) light delivered by an argon laser-pumped dye laser (Spectra Physics, Mountain View, CA) as previously described [6,13]. Colo26 tumor bearing mice were treated with either 88 or 48 J/cm^2 given at 14 mW/cm^2. 4T1 tumor bearing mice were treated with 88 J/cm^2 given at 20 mW/cm^2. Control groups included mice that were either treated with photosensitizer or light alone, or received no treatment.

Neutrophil Detection

The number of neutrophils present in the blood was determined microscopically. Peripheral blood was collected from untreated and PDT-treated animals at various times posttreatment. Blood smears were prepared on microscope slides and cells were fixed by treatment with 95% ethyl alcohol. Slides were stained with Wright–Giemsa stain and the number of segmented, mature neutrophils/ml was determined microscopically. Each slide was counted at least twice and a minimum of 100 cells/slide/analysis were examined.

The number of neutrophils present in bone marrow, tumor, and tumor draining lymph node (TDLN) was determined by flow cytometry. Femurs were isolated from untreated and PDT-treated mice at various times postPDT. Bone marrow cells were harvested by flushing each femur with phosphate buffered saline; RBC were removed by treatment with ammonium chloride. RBC-depleted cells were suspended in PAB buffer (HBSS without $Ca^{2+}Mg^{2+}$ containing 5 mg/ml BSA). Single cell suspensions were generated from tumors as previously described [20]. Briefly, tumors were disaggregated in HBSS containing collagenase (type II, Worthington Biochemical Corp., Freehold, NJ) and BSA. Single cell suspensions were generated from TDLNs by mechanical disruption using a tissue sieve. RBC were depleted from both tumor and TDLN single cell suspensions and the RBC-depleted cells were suspended in PAB.

Cells were stained with a panel of monoclonal antibodies (mAb) to detect specific cell-surface antigens (CD11b, Gr1, and F4/80), as previously described [6]. The mAbs were directly conjugated with the following fluorochromes: Fluorescein (FITC), phycoerythrin (PE), PerCPCy5.5, and allophycocyanin (APC) (all from Phar-Mingen, except F4/80, which was purchased from e-bioscience). A BD FACSCalibur was used for flow cytometric analysis; data was acquired from 200,000 cells stored in collateral list mode and analyzed using the WinList processing program (Verity Software House, Inc.). For the determination of the absolute number of specific cell populations, the percentage of each population was multiplied by the number of cells recovered from the respective tumor or TDLN.

Cytokine Analysis

Tumors and TDLNs were harvested at the indicated time points and flash frozen on dry ice. Tissue was homogenized in CelLytic™MT from Sigma (Saint Louis, MO) containing protease inhibitor cocktail (Sigma, St. Louis, MO); protein concentration of the lysate was determined using the Bio-Rad Protein Assay (Bio-Rad Laboratories, Hercules, CA). ELISA kits specific for KC, MIP2, and IL-6 were purchased from R&D systems (Minneapolis, MN) and used according to the manufacturer's instructions. The results were normalized to per μg total protein.

T-Cell Activation

T-cell activation was determined by assessing the phenotype of T cells present in the TDLN after PDT using flow cytometry [6]. Axillary TDLNs were harvested at the indicated time points and single-cell suspensions were generated. Cells were stained with a panel of mAb to detect specific cell-surface antigens (CD8 and CD44), as previously described [20]. The mAbs were directly conjugated with the following fluorochromes: FITC, PE, PerCPCy5.5, and APC (all from PharMingen). A BD FACSCalibur was used for flow cytometric analysis; data was acquired from 200,000 TDLN cells stored in collateral list mode and analyzed using the WinList processing program (Verity Software House, Inc.). For the determination of the absolute number of specific cell populations, the percentage of each population was multiplied by the number of cells recovered from the respective TDLN.

Assessment of Tumor Response

Following treatment, orthogonal diameters of tumors were measured once every 2 days with calipers. The tumor volume, V, was calculated with the formula $V = (lw^2/2)$, were l is the longest axis of the tumor and w is the axis perpendicular to l. The tumors were monitored until they reached a volume greater than 400 mm^3, at which time the mice were euthanized. No tumor regrowth was ever observed later than ~day 50 and therefore animals were considered cured if they remained tumor free for at least 60 days after PDT.

Photosensitizer Concentration in Tumors

Photosensitizer uptake in tumor tissue was determined using ^{14}C-labeled HPPH or by fluorescence 24 hours after a single i.v. injection of drug as described [26,27]. HPPH uptake by tumors was determined by administration of ^{14}C-labeled HPPH (0.2 ml/5 μCi) to tumor bearing mice; 24 hours following injection tumors were collected, weighed and placed in 1 ml of Solvable (Packard Instruments) and heated to 53°C in the dark for 16–18 hours. Samples were cooled and bleached by addition of 80 μl of bleach. Radioactivity was determined after addition of Ultima Gold scintillation fluid. To determine sodium Porfimer uptake 50 mg of tumor was placed in 1 ml of Solvable and heated to 53°C in the dark for 16–18 h. Samples were cooled and fluorescence spectra with λ_{ex} = 406 nm and λ_{em} = to 627 nm. Drug concentrations were calculated by comparing experimental fluorescence intensities to internal standards obtained by spiking samples with known amounts of drug immediately before solubilization.

Western Analysis

The analysis of STAT3 cross-linking by PDT was performed as described [28]. Briefly tumor tissue was collected immediately after PDT and homogenized in radioimmunoprecipitation assay buffer [29]. Protein extracts were separated on 6% SDS-polyacrylamide gels and transferred to PDVF membranes (Hybond-P, Amersham Pharmacia Biotech, Piscataway, NJ). Membranes were then reacted overnight at 4°C with antibodies to STAT3 (Santa Cruz Biotechnology, Santa Cruz, CA), phosphotyrosine-STAT3 (New England Biolabs, Inc., Ipswich, MA), or Bax (Santa Cruz Biotechnology). Detection of the

immune complexes was done using peroxidase-coupled secondary antibodies and enhanced chemiluminescence detection (Pierce Chemical, Rockford, IL). Luminescence was detected using a Molecular Imager Gel Doc XR+ System (Bio-Rad Laboratories). Images were quantified using Image Lab software (Bio-Rad); the ability of PDT to cross-link STAT3 was expressed as the percentage conversion of monomeric STAT3 into oligomers.

Immunohistochemistry

Immunohistochemistry was performed as described [8]. Briefly, tumors harvested with overlying and adjacent skin were immediately placed in Tris- buffered zinc fixative (0.1 M Tris HCl buffer at pH 7.4 containing 3.2 mM calcium acetate, 22.8 mM zinc acetate and 36.7 mM zinc chloride), transferred to 70% ethanol, dehydrated and embedded in paraffin. Sectioning and staining was carried out by the Roswell Park Cancer Institute Pathology Resource using routine immunohistochemical methods [8]. Caspase 3 was detected with rabbit IgG specific for caspase 3 (Cell Signaling Tech., Danvers, MA). Apoptosis was detected using the Apoptag® Plus Peroxidase *in situ* Detection Kit (Chemicon International, Inc. Temecula, CA), which labels single and double stranded DNA breaks by the TUNEL (Terminal deoxynucleotidyl transferase-mediated d-UTP Nick End Labeling) method. Positive staining cells appear as brown cells. Slides were counterstained with hematoxylin, which results in the nuclei appearing blue.

Colony Forming Assays

Tumors were harvested at various times following PDT and single cell suspensions were generated by digestion with pronase, DNase I, and collagenase [30]. Cell viability was determined by trypan blue exclusion. Appropriate numbers of tumor cells were plated in 100-cm dishes in growth media. Dishes were incubated in the dark in a humidified atmosphere of 5% CO_2 for 7–9 days at which time the cultures were fixed, stained, and macroscopic colonies were counted. Clonogenicity was determined by multiplying the number of viable cells/g of tissue by the plating efficiency, which is determined by dividing the number of colonies observed by the number of cells seeded in the assay.

Statistical Evaluation

All measured values are presented as means ± SEM (standard error of the mean). The one-tailed Student's *t*-test was used for comparison between groups in all experiments except for tumor response determinations. For tumor response data analysis, hours-to-event, i.e., to 400 mm^3 tumor volume, was calculated for each animal by linearly interpolating between the times just before and after this volume was reached, using log (tumor volume) for the calculations; both tumor volume and hours-to-event calculations were performed using Excel™ (Microsoft, Redmond,WA). Tumor responses between groups were compared using the Kaplan–Meier analysis [8].

RESULTS

IL-6 Does Not Control Inflammation Post-PDT

PDT induced inflammation is characterized by (i) infiltration of neutrophils into the treated tumor bed and TDLN and (ii) increases in proinflammatory cytokine expression [7,8,19]. Blood, bone marrow, tumor, and TDLN were examined for the presence of neutrophils following HPPH-PDT of Colo26 tumors grown in BALB/c or $IL6^{-/-}$ mice. Neutrophils were characterized morphologically in the blood. Bone marrow, tumor, and TDLN infiltrating neutrophils were defined by expression of CD45, CD11b, and Gr1 in the absence of the macrophage marker F4/80. The number of neutrophils present in the blood significantly increased within 4 hours of HPPH-PDT of Colo26 tumors in BALB/c mice and

remained high up to 8 hours after treatment ($P \leq 0.001$; Fig. 1A). In contrast there was no significant change in the number of systemic neutrophils following PDT of *IL6*$^{-/-}$ tumor bearing mice, suggesting that IL-6 plays a role in neutrophil release from the bone marrow. This hypothesis was confirmed by examination of the bone marrow posttreatment. Treatment of tumor bearing BALB/c mice led to a significant reduction in the number of neutrophils present in the bone marrow at 4 and 8 hours post-PDT that was the inverse of the increase in circulating neutrophils ($P \leq 0.01$; Fig. 1B). With the exception of the 8-hour time point, no significant reduction in neutrophil number was observed in the bone marrow of *IL6*$^{-/-}$ tumor bearing mice following PDT. HPPH-PDT of Colo26 tumors resulted in accumulation of neutrophils in the treated tumor and TDLN regardless of the strain of mouse (Fig. 1C/D).

PDT treatment of Colo26 tumors in both BALB/c and *IL6*$^{-/-}$ mice resulted in significant increases in expression of the proinflammatory cytokines, KC, and MIP-2 at all time points examined ($P \leq 0.01$; Fig. 2A/B). Treatment of tumors in BALB/c mice leads to a characteristic increase in IL-6 and a small but significant increase in IL-6 expression *IL6*$^{-/-}$ mice (Fig. 2C). The source of IL-6 in *IL6*$^{-/-}$ was likely the tumor cells themselves as there is no corresponding increase in systemic levels of IL-6 (Fig. 2D) or expression of IL-6 in the TDLN (data not shown).

IL-6 Inhibits PDT Enhancement of Immune Memory

We next investigated the effect of IL-6 on PDT enhancement of T-cell activation and antitumor immunity. TDLNs were collected from Colo26 BALB/c and *IL6*$^{-/-}$ tumor bearing mice treated with HPPH only or with HPPH-PDT at various time points posttreatment. The number of activated CD8$^+$ T cells per TDLN was determined by flow cytometric analysis; activated CD8$^+$ T cells were defined by expression of high levels of CD44 [6]. PDT of Colo26 tumors in both strains of mice led to significantly increased numbers of activated CD8$^+$ T cells 1 day after treatment (Fig. 3A; $P \leq 0.01$ as compared to 0 hour); although the number of activated CD8$^+$ T cells following PDT was significantly lower in *IL6*−/− mice one day post-PDT as compared to that observed in BALB/c mice ($P \leq 0.01$). However, by day 2, the number of activated CD8$^+$ T cells present in TDLN following PDT was equivalent in BALB/c and *IL6*$^{-/-}$ mice. When T-cell activation was further defined by coexpression of the early activation markers CD69 and CD25, similar results were observed (data not shown).

To determine the effect of IL-6 on formation of immune memory, splenocytes were isolated from BALB/c and *IL6*$^{-/-}$ mice whose Colo26 tumors had been eradicated by PDT and who remained tumor free for at least 60 days. The splenocytes were depleted of myeloid cells by adherence and transferred to naïve SCID mice. Recipient mice were challenged by i.v. injection with live tumor cells. Lung tissue was isolated 18 days after challenge and examined for the presence of lung tumors. Adoptive transfer of splenocytes isolated from BALB/c or *IL6*$^{-/-}$ mice significantly inhibited lung tumor formation in the recipient mice when compared to control mice (Fig. 3B; $P \leq 0.001$). Additionally, significantly fewer lung tumors were found in PDT treated and cured *IL6*$^{-/-}$ mice when compared to cured BALB/c mice ($P \leq 0.05$).

IL-6 Potentiates Tumor Resistance to PDT

IL-6 has been shown to either have no effect or enhance PDT efficacy [19,22,31]. In those studies IL-6 was blocked using neutralizing antibodies or by administration of soluble gp130, which inhibits IL-6 trans-signaling; thus the observed differences in the results could be due to incomplete neutralization or inhibition. Therefore we tested tumor responses in BALB/c and *IL6*$^{-/-}$ mice. To ensure that the observed results were not tumor specific, the

effect of IL-6 on tumor response to PDT was tested in two different tumor models: Colo26, a murine colon carcinoma (Fig. 4A) and 4T1 (Fig. 4B), a murine mammary carcinoma. In each tumor model system, the tumor growth kinetics were marginally, but not significantly, delayed in the absence of IL-6. The response of Colo26 tumors to HPPH-PDT has been well-characterized [8]. The increase in immune memory observed in the absence of IL-6 suggested that PDT efficacy may increase in the absence of IL-6; therefore, Colo26 tumor bearing mice were treated with HPPH-PDT at two suboptimal doses, 88 J/cm^2 and 48 J/cm^2. Similarly, 4T1 tumor bearing mice were treated with a suboptimal dose of Porfimer sodium (PII)-PDT (80 J/cm^2), which allowed determination of whether the observed effects were duplicated when another photosensitizer was used. The Colo26 tumor response to HPPH-PDT significantly increased in the absence of IL-6 regardless of treatment dose ($P \leq 0.03$). The 4T1 tumor response also improved from 30% tumor-free mice to 77% in the absence of IL-6 ($P \leq 0.02$). Photosensitizer uptake was equivalent in tumors grown in BALB/c and *Il6*$^{-/-}$ mice (Fig. 4C).

Bone marrow chimeras were generated to determine whether IL-6 expression in hematopoietic or nonhematopoietic cells was required for increase tumor resistance to PDT. Bone marrow from BALB/c (wt) or *IL6*$^{-/-}$ mice was adoptively transferred to lethally irradiated recipient mice 9 weeks after reconstitution. Colo26 tumor bearing reconstituted recipient mice were treated with HPPH-PDT and the tumor response was followed for 60 days. The Colo26 tumor response to HPPH-PDT was significantly lower in animals expressing IL-6 in either the hematopoietic or nonhematopoietic cellular compartment ($P \leq 0.003$; Fig. 4C). Thus, it appears that IL-6 expression in the tumor microenvironment, regardless of cellular source, is sufficient for increased tumor resistance to PDT.

It is possible that the increased PDT efficacy observed in *IL6*$^{-/-}$ mice is a result of differences in the delivered PDT dose. PDT dose is correlated with the degree of STAT3 cross-linking present immediately after PDT [28,29]. The degree of STAT3 cross-linking observed immediately following PDT of Colo26 tumors was similar regardless of the mouse strain (Fig. 5A/B) suggesting that equivalent PDT dose was delivered to tumors grown in both strains of mice.

IL-6 Enhances Tumor Survival

IL-6 has been shown to stimulate the expression of survival proteins and inhibit apoptosis [32]; improved tumor response to PDT in the absence of IL-6 could be the result of decreased tumor survival. The degree of direct cell death induced by PDT was determined using colony formation assays. The colonogenicity of Colo26 and 4T1 tumor cells isolated from tumors grown in BALB/c and *IL6*$^{-/-}$ mice immediately after PDT was not significantly different (Fig. 6A). The tissue sections were isolated 3 hours after PDT and then stained with ApoTag indicates that similar levels of apoptosis between tumors grown in BALB/c and IL6KO mice (Fig. 6B). However, Colo26 tumor sections isolated 24 hours post-PDT from *IL6*$^{-/-}$ mice appear to show a greater Caspase 3 expression when compared to those isolated from BALB/c mice (Fig. 6C); similarly there was a decrease in surviving cells present in the tumors isolated from *IL6*$^{-/-}$ mice 24 hours after PDT (Fig. 6D) The increase in apoptosis was further confirmed by analysis of expression of the proapoptotic protein Bax in Colo26 tumor cell lysates isolated from BALB/c or *IL6*$^{-/-}$ mice following HPPH-PDT. Tumor lysates from *IL6*$^{-/-}$ mice have higher levels of Bax as compared to tumor lysates isolated from BALB/c mice (Fig. 6E). These studies suggest that although IL-6 does not contribute to direct tumor cell kill by PDT, it may contribute to long-term tumor cell survival by inhibiting apoptosis.

DISCUSSION

IL-6 is a pluripotent cytokine that has previously been shown to play a major role in T-cell proliferation, survival, and function [15]. Clinical and preclinical studies have shown that PDT of tumors can lead to local and systemic induction of IL-6 [8,16–20] and enhanced T-cell mediated antitumor immunity [6,7,9,33]. In this study we examined the role of IL-6 in PDT induced antitumor immunity. Our results demonstrate that IL-6 does not contribute to primary antitumor T-cell activation but does appear to impair the generation of antitumor immunity by PDT. Examination of effect of IL-6 on PDT efficacy showed that long-term tumor growth control by PDT was significantly inhibited by IL-6 in two murine carcinoma models, Colo26 colon carcinoma and 4T1 mammary carcinoma. The decreased efficacy appears to be due, at least in part, to an IL-6 dependent inhibition in expression of the proapoptotic protein, Bax.

Although the failure to demonstrate a role for IL-6 in PDT activation of primary T cells and generation of antitumor immunity is somewhat surprising, it is not unprecedented. PDT induced antitumor immunity is largely mediated by $CD8^+$ T cells [5,7,13] and can be generated in the absence of $CD4^+$ T cell help [13]. A recent study by Longhi et al. [34] showed that primary and memory $CD8^+$ T-cell response to influenza are unimpaired in *IL6*$^{-/-}$ mice. Similarly, Kopf et al. [24] reported that $CD4^+$ independent $CD8^+$ T-cell responses were identical in wild type and *IL6*$^{-/-}$ mice. Furthermore, $CD8^+$ T-cell activation following PDT is dependent upon neutrophil mobilization into the treated tumor and/or TDLN [6], which was not impaired in the absence of IL-6.

IL-6 mediates its activity through interaction with a heterotrimeric membrane-associated receptor [35]. The IL-6 receptor (IL-6R) complex is made of a ligand binding subunit (IL-6Rα/gp80) and two signaling subunits (IL-6Rβ/gp130). IL-6Rα exists in both membrane and soluble forms; the soluble form, referred to as sIL-6R, binds to IL-6 and promotes interaction with gp130 and subsequent signal transduction. This signaling mechanism is referred to as “trans-signaling”. IL-6 classical signaling and trans-signaling pathways lead to activation of multiple intracellular signaling pathways, including the signal transducer and activator of transcription (STAT)-3, MAP kinase, and phosphoinositol 3 kinase (PI3K) pathways. Previous studies have shown that IL-6/STAT3 promote the expression of numerous prosurvival and antiapoptotic proteins [32]. Over-expression of IL-6 in human basal cell carcinoma cell lines has also been shown to increase expression of the antiapoptotic protein Mcl-1 and increase resistance to PDT [36]. However, Usuda et al. [37] showed that Lewis lung carcinoma cells over-expressing IL-6 exhibited increased sensitivity to PDT that may have been due to increased expression of the proapoptotic Bax protein. In the current study we observed that PDT did not lead to a loss of Bax expression in the absence of IL-6, which may have lead to the increase PDT efficacy observed in this study. This may indicate a tumor specific response to PDT; however it is important to note that our studies examined the response to PDT induced IL-6 expression *in vivo* as opposed to the response of PDT treated genetic engineered cell lines *in vitro*.

Most striking was the finding that IL-6 significantly inhibited PDT efficacy in treatment of both Colo26 and 4T1 tumors. Previous studies in our laboratory failed to demonstrate a role for IL-6 in the response of EMT6 murine mammary tumors to HPPH-PDT [19]. Similarly, Sun et al.[21] did not observe changes in the response of SCCVII tumors to mTHPC-based PDT when IL-6 was blocked by administration of neutralizing antibodies. In both our previous studies and those of Sun et al., IL-6 neutralizing antibodies were administered short term, either immediately before PDT or immediately before and 24 hours post PDT. Tumor response was then followed for at least 60 days. It is possible that the discrepancy between

our current study and the previous studies is due to incomplete blocking of PDT-induced IL-6 or the short duration of blocking. In the current study, IL-6 was permanently blocked.

The differences in findings may also indicate that the effect of IL-6 on long-term tumor growth control by PDT may be tumor specific. However, Wei et al. [22] showed that the Colo26 response to HPPH-PDT was inhibited by sgp130, which blocks IL-6 trans-signaling, and enhanced by hyper IL-6, which enhances IL-6 trans-signaling. Ours is the first study to examine the role of IL-6 in tumor response to PDT using $IL6^{-/-}$ mice, which lack both classical and trans-signaling IL-6 pathways. The difference in results between our study and those of Wei et al. [22] could be due to differences in the role of IL-6 classical and trans-signaling in the tumor response to PDT. In studies examining the role of IL-6 in sepsis, inhibition of IL-6 trans-signaling rescued mice more effectively than global IL-6 blockade [38,39]. This was thought to be due to the fact that in the absence of classical IL-6 signaling, as would occur in mice IL-6, epithelial cells were less likely to proliferate and regenerate. A similar scenario could be occurring in the tumor response to PDT such that in total loss of IL-6, as occurs in $IL6^{-/-}$ mice, IL-6 protection of tumor cells would be lost, leading to increased PDT efficacy.

PDT efficacy and ability to induce inflammation is strongly influenced by treatment parameters, such as fluence rate. Henderson et al. [40] showed that high fluence, given at low fluence rate, induced minimal inflammation and low expression of IL-6, but was highly effective. In contrast treatments of lower fluence, also given at low fluence rates, induced maximal inflammation and high levels of IL-6, but suboptimal cure rates. Given these findings it is likely that tumor cure rates following optimal PDT regimens will not be enhanced by depletion of IL-6; and that the low levels of IL-6 induced by these treatment regimes will not affect antitumor immunity.

PDT efficacy following suboptimal, inflammation inducing PDT was dependent upon neutrophils infiltration into secondary tissues, including the tumor [8]. In both the current study and our previous study [19], we show that neutrophil migration into secondary tissue is independent of IL-6. These findings suggest that the effect of IL-6 on the efficacy of suboptimal, inflammation inducing IL-6 not mediated by an effect on neutrophil migration.

In this study we employed two photosensitizers, HPPH, and Porfimer sodium, both of which work largely by targeting tumor cells [41]. A recent study by Preise et al. [42] demonstrated that vascular-targeted PDT induced strong inflammation and systemic antitumor immunity. Vascular-targeted PDT also induced a substantial humoral immune response that was effective at controlling tumor growth when transferred to naïve mice. Although the authors did not specifically examine the ability of vascular-targeted PDT to induce IL-6, the presence of activated neutrophils in the treated tumor bed, suggests that this treatment induces inflammation and will result in enhanced IL-6 production. IL-6 plays a critical role in B-cell differentiation and activation [43] and it is unclear what role IL-6 has in the efficacy of vascular-targeted PDT.

The development of PDT regimens that enhance antitumor immunity and potentially combat disease present outside the treatment field has led to proposals for the use of PDT as an adjuvant treatment in treatment of metastases. However, our results show that the potential for PDT induced expression of IL-6 to promote tumor cell proliferation and survival must be taken into account.

Acknowledgments

The authors would like to thank Dr. David Bellnier for his input into the writing of this publication. The work was supported by NIH Grants CA55791 and CA98156 and in part by the Roswell Park Cancer Center Support Grant CA16056.

Contract grant sponsor: NIH; Contract grant numbers: CA55791; CA98156; Contract grant sponsor: Roswell Park Cancer Center Support Grant; Contract grant number: CA16056.

REFERENCES

1. Brown SB, Brown EA, Walker I. The present and future role of photodynamic therapy in cancer treatment. Lancet Oncol. 2004; 5:497–508. [PubMed: 15288239]
2. Henderson, BW.; Gollnick, SO. Mechanistic principles of photodynamic therapy. In: Vo-Dinh, T., editor. Biomedical photonics handbook. CRC Press; Boca Raton, FL: 2003. p. 36-1-36-27.
3. MacDonald IJ, Dougherty TJ. Basic principles of photodynamic therapy. J Porphyrins Phthalocyanines. 2001; 5:105–129.
4. Gollnick SO, Owczarczak B, Maier P. Photodynamic therapy and anti-tumor immunity. Lasers Surg Med. 2006; 38:509–515. [PubMed: 16788921]
5. Gollnick SO, Brackett CM. Enhancement of anti-tumor immunity by photodynamic therapy. Immunol Res. 2010; 46:216–226. [PubMed: 19763892]
6. Kousis PC, Henderson BW, Maier PG, Gollnick SO. Photodynamic therapy (PDT) enhancement of anti-tumor immunity is regulated by neutrophils. Cancer Res. 2007; 67:10501–10510. [PubMed: 17974994]
7. Castano AP, Mroz P, Hamblin MR. Photodynamic therapy and anti-tumour immunity. Nat Rev Cancer. 2006; 6:535–545. [PubMed: 16794636]
8. Henderson BW, Gollnick SO, Snyder JW, Busch TM, Kousis PC, Cheney RT, Morgan J. Choice of oxygen-conserving treatment regimen determines the inflammatory response and outcome of photodynamic therapy of tumors. Cancer Res. 2004; 64:2120–2126. [PubMed: 15026352]
9. Kabingu E, Oseroff AR, Wilding GE, Gollnick SO. Enhanced systemic immune reactivity to a basal cell carcinoma associated antigen following photodynamic therapy. Clin Cancer Res. 2009; 15:4460–4466. [PubMed: 19549769]
10. Korbelik M. Induction of tumor immunity by photodynamic therapy. J Clin Laser Med Surg. 1996; 14:329–334. [PubMed: 9612200]
11. Korbelik M, Cecic I. Contribution of myeloid and lymphoid host cells to the curative outcome of mouse sarcoma treatment by photodynamic therapy. Cancer Lett. 1999; 137:91–98. [PubMed: 10376798]
12. de Vree WJ, Essers MC, De Bruijn HS, Star WM, Koster JF, Sluiter W. Evidence for an important role of neutrophils in the efficacy of photodynamic therapy *in vivo*. Cancer Res. 1996; 56:2908–2911. [PubMed: 8674038]
13. Kabingu E, Vaughan L, Owczarczak B, Ramsey KD, Gollnick SO. $CD8^+$ T cell-mediated control of distant tumours following local photodynamic therapy is independent of $CD4^+$ T cells and dependent on natural killer cells. Br J Cancer. 2007; 96:1839–1848. [PubMed: 17505510]
14. Rose-John S, Scheller J, Elson G, Jones SA. Interleukin-6 biology is coordinated by membrane-bound and soluble receptors: Role in inflammation and cancer. J Leukoc Biol. 2006; 80:227–236. [PubMed: 16707558]
15. Jones SA. Directing transition from innate to acquired immunity: Defining a role for IL-6. J Immunol. 2005; 175:3463–3468. [PubMed: 16148087]
16. Korbelik M, Cecic I, Merchant S, Sun J. Acute phase response induction by cancer treatment with photodynamic therapy. Int J Cancer. 2008; 122:1411–1417. [PubMed: 18033689]
17. Du H, Bay BH, Mahendran R, Olivo M. Hypericin-mediated photodynamic therapy elicits differential interleukin-6 response in nasopharyngeal cancer. Cancer Lett. 2006; 235:202–208. [PubMed: 15935550]
18. Yom SS, Busch TM, Friedberg JS, Wileyto EP, Smith D, Glatstein E, Hahn SM. Elevated serum cytokine levels in mesothelioma patients who have undergone pleurectomy or extrapleural

pneumonectomy and adjuvant intraoperative photodynamic therapy. Photochem Photobiol. 2003; 78:75–81. [PubMed: 12929752]

19. Gollnick SO, Evans SE, Baumann H, Owczarczak B, Maier P, Vaughan L, Wang WC, Unger E, Henderson BW. Role of cytokines in photodynamic therapy-induced local and systemic inflammation. Br J Cancer. 2003; 88:1772–1779. [PubMed: 12771994]
20. Gollnick SO, Liu X, Owczarczak B, Musser DA, Henderson BW. Altered expression of interleukin 6 and interleukin 10 as a result of photodynamic therapy *in vivo*. Cancer Res. 1997; 57:3904–3909. [PubMed: 9307269]
21. Sun J, Cecic I, Parkins CS, Korbelik M. Neutrophils as inflammatory and immune effectors in photodynamic therapy-treated mouse SCCVII tumours. Photochem Photobiol Sci. 2002; 1:690–695. [PubMed: 12665307]
22. Wei LH, Baumann H, Tracy E, Wang Y, Hutson A, Rose-John S, Henderson BW. Interleukin-6 trans signalling enhances photodynamic therapy by modulating cell cycling. Br J Cancer. 2007; 97:1513–1522. [PubMed: 17987036]
23. Kopf M, Le Gros G, Coyle AJ, Kosco-Vilbois M, Brombacher F. Immune responses of IL-4, IL-5, IL-6 deficient mice. Immunol Rev. 1995; 48:45–69. [PubMed: 8825282]
24. Kopf M, Baumann H, Freer G, Freudenberg M, Lamers M, Kishimoto T, Zinkernagel R, Bluethmann H, Kohler G. Impaired immune and acute-phase responses in interleukin-6-deficient mice. Nature. 1994; 368:339–342. [PubMed: 8127368]
25. Aslakson CJ, Miller FR. Selective events in the metastatic process defined by analysis of the sequential dissemination of subpopulations of a mouse mammary tumor. Cancer Res. 1992; 52:1399–1405. [PubMed: 1540948]
26. Bellnier DA, Henderson BW, Pandey RK, Potter WR, Dougherty TJ. Murine pharmacokinetics and antitumor efficacy of the photodynamic sensitizer 2-[1-hexyloxyethyl]-2-devinyl pyropheophorbide-a. J Photochem Photobiol B. 1993; 20:55–61. [PubMed: 8229470]
27. Bellnier DA, Greco WR, Parsons JC, Oseroff AR, Kuebler A, Dougherty TJ. An assay for the quantitation of Photofrin in tissues and fluids. Photochem Photobiol. 1997; 66:237–244. [PubMed: 9277143]
28. Henderson BW, Daroqui C, Tracy E, Vaughan LA, Loewen GM, Cooper MT, Baumann H. Cross-linking of signal transducer and activator of transcription 3–a molecular marker for the photodynamic reaction in cells and tumors. Clin Cancer Res. 2007; 13:3156–3163. [PubMed: 17545518]
29. Liu W, Oseroff AR, Baumann H. Photodynamic therapy causes cross-linking of signal transducer and activator of transcription proteins and attenuation of interleukin-6 cytokine responsiveness in epithelial cells. Cancer Res. 2004; 64:6579–6587. [PubMed: 15374971]
30. Henderson BW, Waldow SM, Mang TS, Potter WR, Malone PB, Dougherty TJ. Tumor destruction and kinetics of tumor cell death in two experimental mouse tumors following Photodynamic Therapy. Cancer Res. 1985; 45:572–576. [PubMed: 3967232]
31. Cecic I, Sun J, Korbelik M. Role of complement anaphylatoxin C3a in photodynamic therapy-elicited engagement of host neutrophils and other immune cells. Photochem Photobiol. 2006; 82:558–562. [PubMed: 16613513]
32. Ara T, Declerck YA. Interleukin-6 in bone metastasis and cancer progression. Eur J Cancer. 2010; 46:1223–1231. [PubMed: 20335016]
33. Thong PS, Ong KW, Goh NS, Kho KW, Manivasager V, Bhuvaneswari R, Olivo M, Soo KC. Photodynamic-therapy-activated immune response against distant untreated tumours in recurrent angiosarcoma. Lancet Oncol. 2007; 8:950–952. [PubMed: 17913664]
34. Longhi MP, Wright K, Lauder SN, Nowell MA, Jones GW, Godkin AJ, Jones SA, Gallimore AM. Interleukin-6 is crucial for recall of influenza-specific memory CD4 T cells. PLoS Pathog. 2008; 4:e1000006. [PubMed: 18389078]
35. Scheller J, Rose-John S. Interleukin-6 and its receptor: From bench to bedside. Med Microbiol Immunol. 2006; 195:173–183. [PubMed: 16741736]
36. Jee SH, Shen SC, Chui HC, Tsai WL, Kuo ML. Overexpression of interleukin-6 in human basal cell carcinoma cell lines increases anti-apoptotic activity and tumorigenic potency. Oncogene. 2001; 20:198–208. [PubMed: 11313947]

37. Usuda J, Okunaka T, Furukawa K, Tsuchida T, Kuroiwa Y, Ohe Y, Saijo N, Nishio K, Konaka C, Kato H. Increased cytotoxic effects of photodynamic therapy in IL-6 gene transfected cells via enhanced apoptosis. Inter J Cancer. 2001; 93:475–480.

38. Barkhausen T, Tschernig T, Rosenstiel P, Van GM, Vonberg RP, Dorsch M, Mueller-Heine A, Chalaris A, Scheller J, Rose-John S, Seegert D, Krettek C, Waetzig GH. Selective blockade of interleukin-6 trans-signaling improves survival in a murine polymicrobial sepsis model*. Crit Care Med. 2011; 39:1407–1413. [PubMed: 21336117]

39. Greenhill CJ, Rose-John S, Lissilaa R, Ferlin W, Ernst M, Hertzog PJ, Mansell A, Jenkins BJ. IL-6 trans-signaling modulates TLR4-dependent inflammatory responses via STAT3. J Immunol. 2011; 186:1199–1208. [PubMed: 21148800]

40. Belicha-Villanueva A, Blickwedehl J, McEvoy S, Golding M, Gollnick SO, Bangia N. What is the role of alternate splicing in antigen presentation by major histocompatibility complex class I molecules? Immunol Res. 2010; 46:32–44. [PubMed: 19830395]

41. Agostinis P, Berg K, Cengel KA, Foster TH, Girotti AW, Gollnick SO, Hahn SM, Hamblin MR, Juzeniene A, Kessel D, Korbelik M, Moan J, Mroz P, Nowis D, Piette J, Wilson BC, Golab J. Photodynamic therapy of cancer: An update. CA Cancer J Clin. 2011; 61:250–281. [PubMed: 21617154]

42. Preise D, Oren R, Glinert I, Kalchenko V, Jung S, Scherz A, Salomon Y. Systemic antitumor protection by vascular-targeted photodynamic therapy involves cellular and humoral immunity. Cancer Immunol Immunother. 2009; 58:71–84. [PubMed: 18488222]

43. Scheller J, Chalaris A, Schmidt-Arras D, Rose-John S. The pro- and anti-inflammatory properties of the cytokine interleukin-6. Biochim Biophys Acta. 2011; 1813:878–888. [PubMed: 21296109]

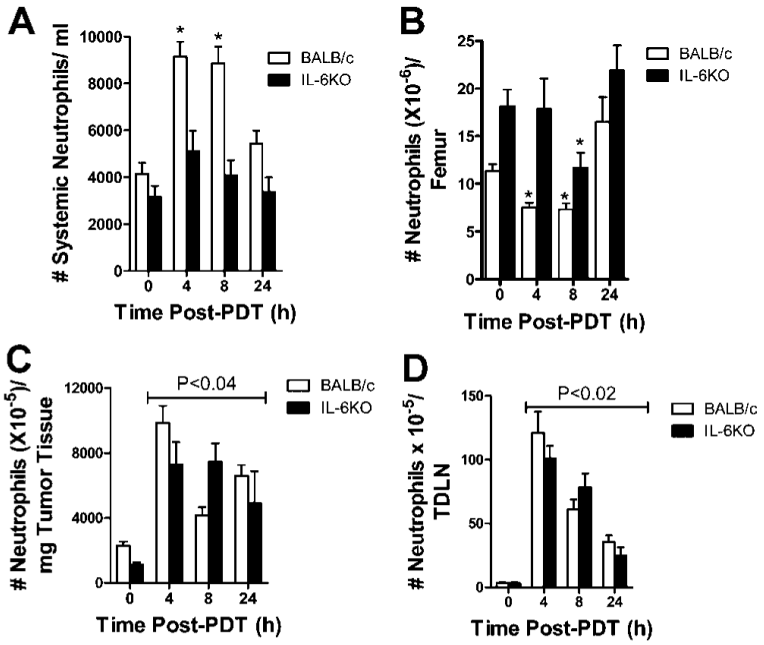

Fig. 1.

IL-6 affects the release of neutrophils from the bone marrow post-PDT, but not neutrophil accumulation in tumor tissue or TDLN. Colo26 tumor bearing BALB/c or *Il6*$^{-/-}$ mice were treated with HPPH-PDT (88 J/cm^2). **A**: Peripheral blood smears were stained with Wright–Giemsa stain and the number of segmented, mature neutrophils/ml was determined microscopically. Results are presented as the # of neutrophils/ml of blood ± SEM; each group contains a minimum of five mice. * indicate values that are significantly different from the value at 0 hour post-PDT; $P \leq 0.001$. **B–D**: The number of neutrophils present in the (B) bone marrow, (C) tumor, and (D) TDLN was determined by flow cytometric analysis. Neutrophils were identified as cells expressing CD11b, high levels (MFI ≥ 10^3) of Gr1 and no F4/80. Results are presented as the average number of neutrophils/tissue ± SEM; each group contains a minimum of six mice. * indicate values that are significantly different from the value at 0 hour post-PDT; $P \leq 0.01$. Lines above indicate that all values are significantly different than the 0 hour time point.

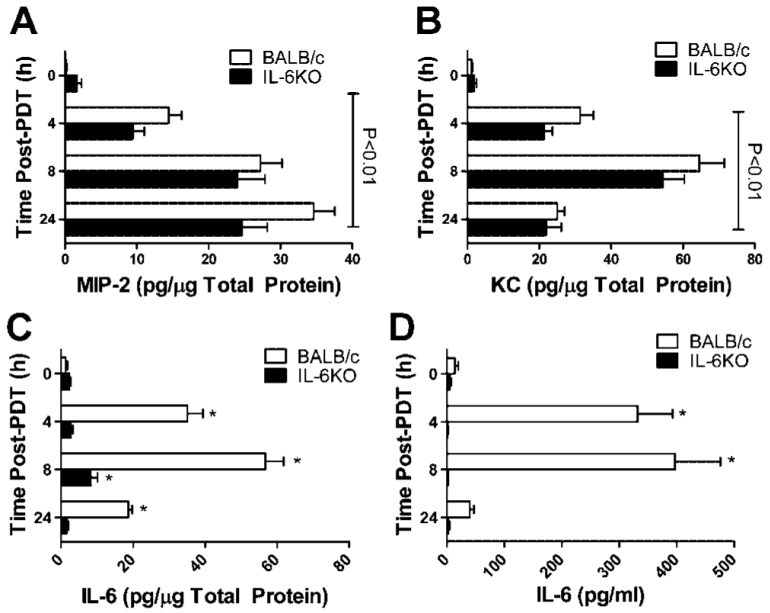

Fig. 2.

IL-6 does not affect the expression of proinflammatory cytokines, MIP2, and KC following PDT. Colo26 tumor bearing BALB/c or *IL6*$^{-/-}$ mice were treated with HPPH-PDT (88 J/cm^2). **A–C**: Tumor tissue was collected at various times post PDT and cytokine specific ELISAs were performed. Results are presented as pg/μg of total protein ± SEM. Each group contains a minimum of six mice. Lines above indicate that all values are significantly different than the 0 hour time point. * indicate values that are significantly different from the value at 0 hour post-PDT; $P \leq 0.02$. **D**: Blood was collected at various times post-PDT and analyzed by ELISA for the presence of IL-6. Results are presented as pg/ml ± SEM; each group contains a minimum of six mice. * indicate values that are significantly different from the value at 0 hour post-PDT; $P \leq 0.001$.

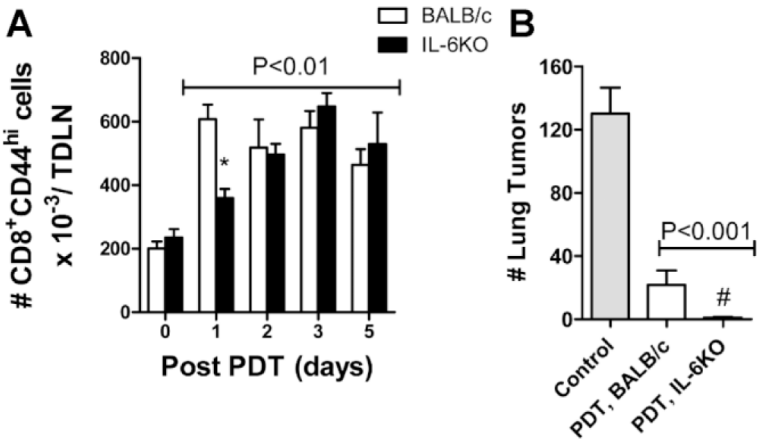

Fig. 3.

IL-6 inhibits PDT enhancement of immune memory. Colo26 tumor bearing BALB/c or *IL6*$^{-/-}$ mice were treated with HPPH-PDT (88 J/cm^2). **A**: Twenty four hours later TDLN were harvested, single cell suspensions generated and the phenotype of CD8$^+$ T cells was determined. The absolute number of CD8$^+$CD44^{Hi} cells/TDLN ±SEM is shown; groups contained a minimum of six mice each. Lines above indicate that all values are significantly different than the 0 hour time point. The asterisk indicates an *IL6*$^{-/-}$ value that is significantly different from that observed in BALB/c mice at that time point; $P \leq 0.01$. **B**: SCID mice were reconstituted with 15×10^6 adherent depleted splenocytes isolated from cured mice 60 days after treatment. Recipient mice were challenged with 10^5 Colo26 cells i.v.; 18 days later lungs were harvested and weighed. Control mice did not receive splenocytes. Groups contained a minimum of five mice each; results are expressed as the average number of lung tumors/mouse ± SEM. Lines above indicate that all values are significantly different than the Control. # indicates a value significantly lower than the number of lung tumors present in recipient mice receiving splenocytes from PDT treated BALB/c mice; $P \leq 0.05$.

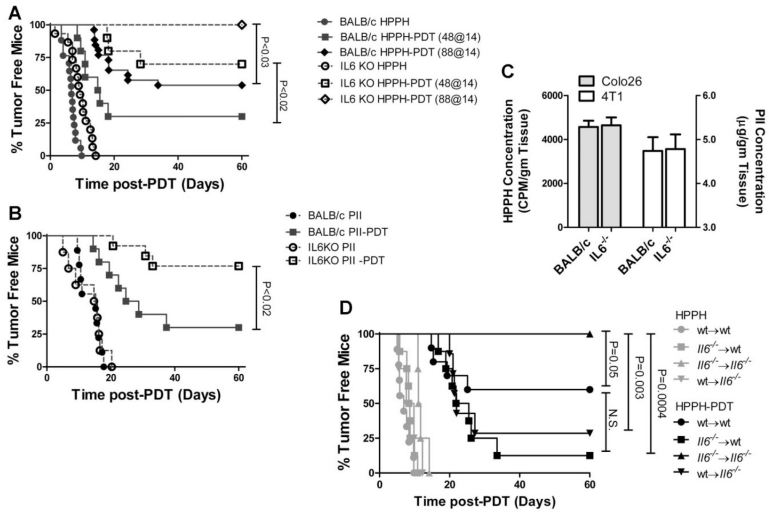

Fig. 4.

IL-6 inhibits PDT efficacy. **A**: Colo26 tumor bearing BALB/c (closed symbols) or *IL6*$^{-/-}$ (open symbols) mice were treated with HPPH alone (circles) or HPPH-PDT at either 48 J/cm^2 (squares) or 88 J/cm^2 (diamonds). Tumor regrowth was followed until the tumors reached 400 mm^3 or for 60 days. Results are reported as the percentage of tumor free mice. Each group contains a minimum of eight mice. **B**: 4T1 tumor bearing BALB/c (closed symbols) or *IL6*$^{-/-}$ (open symbols) mice were treated with Photofrin (PII) alone (circles) or PII-PDT at 88 J/cm^2. Tumor regrowth was followed until the tumors reached 400 mm^3 or for 60 days. Results are reported as the percentage of tumor free mice. Each group contains a minimum of eight mice. **C**: Colo 26 (grey bars) or 4T1 (open bars) tumor bearing BALB/c or IL-6$^{-/-}$ mice were injected with HPPH (Colo 26) or PII (4T1); 24 hours postinjection, tumors were harvested and photosensitizer uptake was determined as described in Material and Methods section. Results are presented as the average photosensitizer concentration/mg of tumor ± SEM; six tumors were examined for each tumor in each strain. **D**: Colo 26 tumor bearing bone marrow chimeric mice were treated with HPPH alone (light symbols) or HPPH-PDT at 88 J/cm^2 (dark symbols). Tumor regrowth was followed until the tumors reached 400 mm^3 or for 60 days. Results are reported as the percentage of tumor free mice. Each group contains a minimum of eight mice.

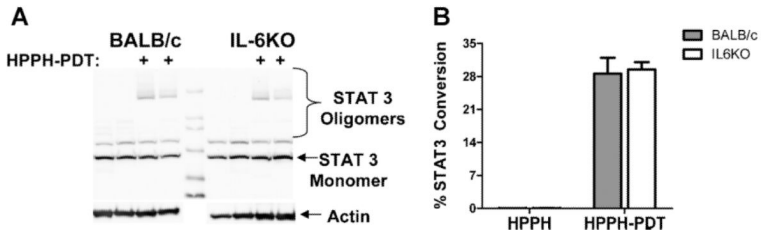

Fig. 5.

PDT dose determination. **A**: Colo26 tumor bearing BALB/c or *IL6*$^{-/-}$ mice were treated with HPPH alone or HPPH-PDT at 88 J/cm^2 (diamonds). Tumors were collected immediately posttreatment and analyzed for the presence of STAT3 crosslinks. A representative gel image is shown. **B**: The degree of cross-linking was determined. Results are presented as the average percentage of conversion of STAT3 monomer to oligomer ± SEM. Two experiments were performed; total of four tumors were analyzed in each strain.

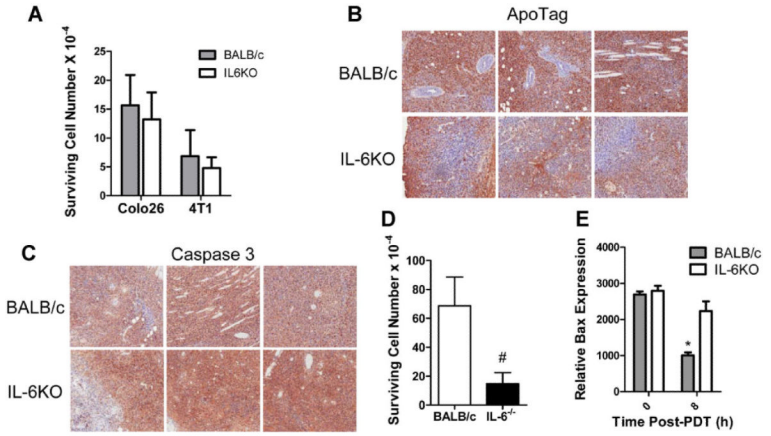

Fig. 6.

IL-6 enhances tumor survival. **A**: Colo26 and 4T1 tumor bearing BALB/c and *IL6*$^{-/-}$ mice were treated with HPPH-PDT (88 J/cm^2) or PII-PDT (88 J/cm^2), respectively. Immediately following treatment tumors were collected and colony forming assays were performed. Results are presented as surviving cell number ± SEM; each bar represents a minimum of five tumors. Each tumor was tested in duplicate. **B–D**: Colo26 tumor bearing BALB/c and *IL6*$^{-/-}$ mice were treated with HPPH-PDT (88 J/cm^2). **B**: 3 hours after treatment, tumors were harvested and analyzed for apoptosis using ApoTag. Representative pictures from each of three tumors are shown. Brown staining indicates the presence of TUNEL$^+$ (apoptotic) cells and the blue counterstain is hematoxalin which stains cell nuclei. C and D: 24 hours after treatment, tumors were harvested and analyzed for (C) apoptosis using a caspase 3 specific antibody or (D) a colony forming assay was performed. Representative pictures from each of three tumors are shown. In (C), brown staining represents the presence of caspase 3$^+$ cells. **E**: Tumors were collected at the indicated time points and analyzed by Western for expression of Bax. The average relative expression present ± SEM in four tumors is shown. * indicates a significant difference from both the 0 hour time point and the 8 hours *IL6*−/− value; $P \leq 0.02$.